Coarsening, Mixing, and Motion: The Complex Evolution of Epitaxial Islands

Yuhai Tu and J. Tersoff

IBM Research Division, T. J. Watson Research Center, P.O. Box 218, Yorktown Heights, New York 10598, USA

(Received 8 November 2006; published 27 February 2007)

During heteroepitaxy, misfit strain causes nanoscale islands to form spontaneously, as ''self-assembled quantum dots.'' The growth and evolution of these islands are remarkably complex. We show that continuum modeling reproduces and explains many of the surprising phenomena observed experimentally. The free energy is reduced by both morphological change and alloy intermixing. However, because diffusion occurs only at the surface, the morphological and compositional evolution are strongly coupled. This leads to a complex dynamical response to the rather simple thermodynamic driving forces.

DOI: 10.1103/PhysRevLett.98.096103 PACS numbers: 68.65.Hb, 68.55.−a, 81.15.Aa

Tremendous effort has been devoted to the study of ''self-assembled quantum dots,'' i.e., three-dimensional Stranski-Krastonov islands that form during strained-layer heteroepitaxy [1]. This work has been driven partly by potential applications in nanoscale technologies such as quantum-dot lasers and memory. An equally important motivation is that island formation exhibits an extraordinarily rich and complex behavior, which is still only partly understood. Thus it provides an ideal test bed to advance our understanding of heteroepitaxial growth in general, and especially the issues that arise in nanoscale structures.

Theoretically, an ultimate goal is to simulate the actual dynamics of nanostructure evolution during growth and processing. While realistic simulations of specific systems are not yet feasible, recently great progress has been made using phase-field modeling [2], three-dimensional continuum modeling [3], and even atomistic simulations [4].

One outstanding issue is the role of intermixing between the deposited material and the substrate. In typical heteroepitaxial systems, there is a large thermodynamic driving force for intermixing, because mixing reduces strain energy and increases entropy [5,6]. Recent experimental work has shown that this intermixing can change the size, shape, and composition of the dots, all of which are crucial factors in any electronic application. Mixing leads to dilution of the quantum dots [7,8] with a nonuniform composition profile [5,9,10]. It can even change the initial nucleation process [11] and cause qualitatively new phenomena such as lateral motion of islands [5,10].

For typical growth times and temperatures, bulk diffusion is negligible in molecular-beam epitaxy, and evolution can occur only by surface diffusion [5,10,12]. However, only recently has a consistent theoretical framework been developed to include such intermixing within a continuum model [13–15]. Applications to date [14–17] have addressed important problems involving nearly planar geometries.

Here we report the first simulation of island evolution that includes intermixing via surface diffusion in the evolution dynamics. This makes it possible to study by direct simulation a broad class of phenomena which previously could be addressed only *ad hoc*. In the absence of bulk diffusion, intermixing can occur only in concert with morphological evolution. We find that this coupling leads to quite rich dynamical behavior in response to the rather simple thermodynamic driving forces.

The simulation automatically produces many of the same phenomena that have been seen experimentally for Ge on Si (001), the most easily studied system. These include trench formation and dilution of the island composition by intermixing with the substrate. We even see a remarkable *lateral motion* of islands leading to asymmetric intermixing, a phenomenon that was only recently discovered experimentally [5,10].

Our continuum approach has been described elsewhere [14,15]. In brief, the system evolves by surface diffusion, while bulk diffusion is assumed to be negligible. Atoms within a few atomic layers of the surface are generally more mobile than in the bulk [15], so we assume that atoms within a depth w_s (perhaps 2–4 monolayers) are in equilibrium with the surface. The free energy of this surface region, $g_s(\xi)$, is a function of ξ, which is the surface composition averaged over the depth w_s. In general, g_s may be different than the bulk free energy function g_b, and any difference drives surface segregation [16]. The composition and morphology evolve as coupled equations:

$$v = \sum_\nu [F_\nu + \nabla \cdot (D_\nu \nabla \mu_\nu)], \tag{1}$$

$$w_s \frac{d\xi_\nu}{dt} = F_\nu + \nabla \cdot (D_\nu \nabla \mu_\nu) - \xi_\nu v. \tag{2}$$

Here the subscript ν labels the two alloy components. F_ν is the incident flux of each component, D_ν is the diffusivity (taken as $\xi_\nu D_{\nu 0}$), and v is the local growth velocity of the surface normal to itself.

We choose parameters based on Ge/Si (001) at 600 °C, insofar as possible [16,18]. The chemical potential μ_ν for each species includes elastic energy, surface energy, and the entropy of mixing [14,15]. (Enthalpy of mixing can be neglected for Ge/Si at typical growth temperatures.) We use an anisotropic surface energy that qualitatively repro-

duces the evolution and shape transitions of Ge on Si (001) [19]. However, the results cannot be compared quantitatively with any specific system, because some crucial properties are not known for any relevant systems. This is especially true of the highly anisotropic surface free energy and its dependence on composition and strain. InAs on GaAs (001) is in many ways similar to Ge/Si [1,20], and our model may be no closer to Ge/Si than Ge/Si is to InAs/GaAs. Still, for convenience we refer to the strained material as "Ge" and the substrate material as "Si."

The surface-energy difference between Ge and Si drives some surface segregation of Ge, which is included here as in Ref. [16]—the alloy is treated as being in local equilibrium over a thickness w_s equivalent to 3 (001) atomic layers, with a lower energy for Ge vs Si in the first atomic layer (i.e., a thickness $w_s/3$ at the surface).

Our simulations are two dimensional, analogous to long island ridges in three dimensions. We treat strain in a low-angle approximation [21], adjusting the surface energy to be prohibitive for angles much steeper than the (105) pyramid. Nevertheless, our results are most comparable to the behavior observed for larger Ge "dome" islands on Si (001). Some of the same phenomena occur in InAs on GaAs (001), and presumably in other systems. The comparisons made to specific experiments are intended only to confirm the existence of the *qualitative* phenomena seen here. We hope that, in the future, a more quantitative understanding of the surface along with full 3D modeling may allow simulations of specific systems with predictive accuracy.

Our results are summarized in Fig. 1, with some key details highlighted in Fig. 2. We first rapidly deposit a thin Ge layer [Fig. 1(a)]. Some intermixing is visible, as well as a thin Ge-rich surface layer due to surface segregation [16]. The system is then allowed to evolve without further deposition. This is somewhat analogous to first depositing a planar layer at low temperature, and then annealing to allow island formation [22].

The substrate was given a slight dimple [23], centered in Fig. 1. Initially, this perturbation triggers the well-known linear instability of a strained layer [24], which spreads laterally. With increasing time [but prior to Fig. 1(b)], 3 and then 5 distinct maxima appear in the growing rippled region, while farther from the initial perturbation the surface remains flat, consistent with Ref. [22]. Soon the entire simulation cell is rippled, with 7 distinct maxima in Fig. 1(b). The ripple maximum located directly over the initial perturbation is the first to form, and it remains the largest throughout the evolution.

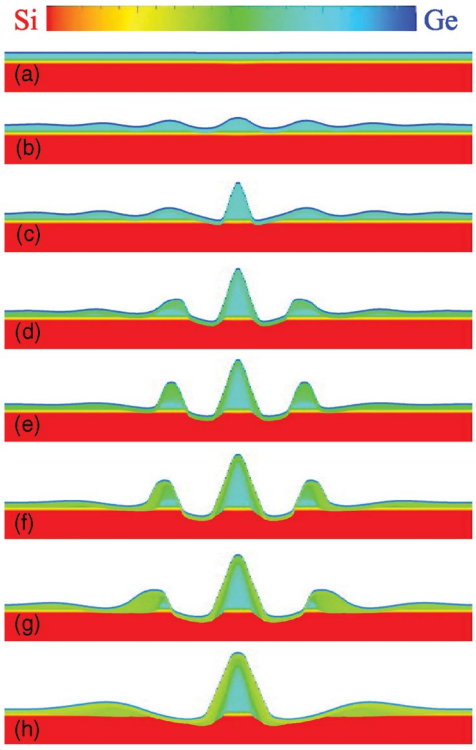

FIG. 1 (color). Selected snapshots from the simulation. Taking the beginning of deposition as $t = 0$, images (a)–(h) correspond to times 3 (end of deposition), 12, 14, 19, 23, 29, 35, and 161, respectively, in arbitrary units. The width of the images is 410 nm, one unit cell of our periodic system. The vertical scale is exaggerated by a factor of ~5. The wetting layer thickness in trough provides a visual marker of w_s (i.e., 0.4 nm) vertically, with the top third enriched by surface segregation. The color bar shows the composition scale.

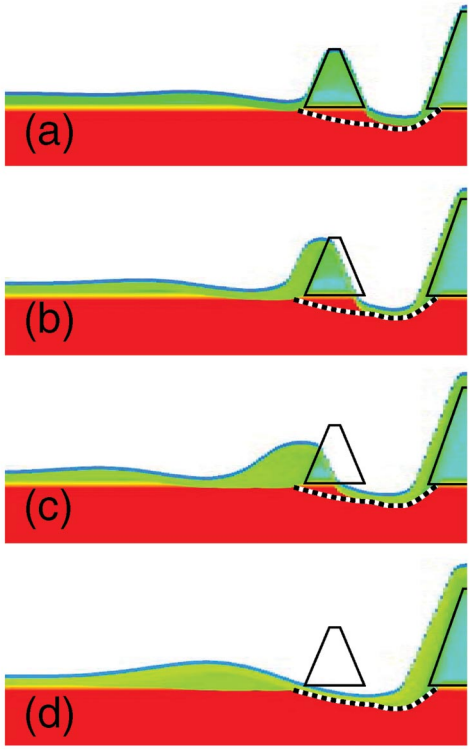

FIG. 2 (color). Expanded view of images (e)–(h) of Fig. 1. Black lines are added outlining the islands in (a) and the trench in (d), and repeated in other panels to help visualize the evolution.

As the ripples increase in amplitude, they pinch off and form distinct islands. Their aspect ratios continue to increase until facets form abruptly on the largest island [Fig. 1(c)] and then on the adjacent islands, due to the surface-energy anisotropy [19]. The facetted islands have much lower chemical potential [19], so they grow rapidly at the expense of the other islands via anomalous coarsening [25]. Thus only the first three islands survive this initial stage of formation, with the first-formed island considerably larger than the others.

This behavior is quite consistent with what is known experimentally about the early stages of island formation. There are experimental indications that, at least under some conditions, islands indeed form by pinch-off and coarsening of more homogeneous ripples [26,27].

Beginning with Fig. 1(c), trenches form around the largest island, digging into the substrate. Strain-driven trench formation has been extensively studied [28–31], and the basic mechanisms are understood. Here we observe the actual formation process. Even as the trench digs deeper into the substrate, it remains lined with a Ge-rich "wetting layer"—bare Si is never exposed. This is also seen experimentally [32]. Figure 2 gives an expanded view, with reference markings to aid in visualizing the evolution. As the island grows in size, it overgrows its own original trench, creating a slope-sided Si mesa centered underneath the island. Just such a structure has recently been seen for Ge/Si [Fig. 2(a) of Ref. [5] and Fig. 5(m) of Ref. [10]].

Once the trench cuts into the substrate, the ejected Si mixes with the Ge being captured by the growing island. As a result, subsequent island growth occurs at a more dilute composition. This is visible as a sharp change in composition between the core and outer layer of the central island after Fig. 1(d) (more visible in Fig. 2). The role of trench formation in providing Si for intermixing was already suggested by Denker *et al.* [5] based on experiment, and here it is seen directly. Note that the large Ge-rich core in Figs. 1 and 2 represents material from the original strained layer that coalesced before the trench reached the substrate. (Such a sharp change in composition seems unlikely to occur in the more common case of nucleation and growth from a continuous flux without postdeposition annealing.)

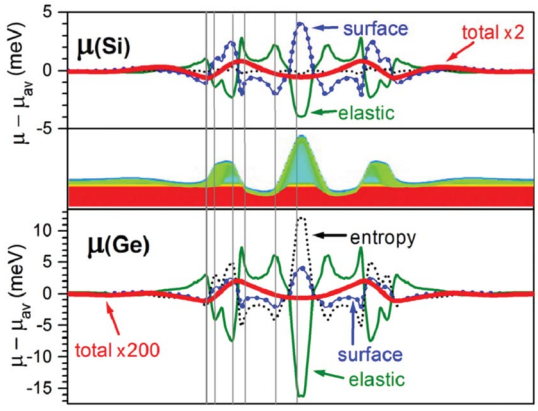

FIG. 3 (color). Variation of chemical potential μ of Si (top panel) and Ge (bottom panel) across the surface, at the time of Fig. 1(f) (middle panel). Elastic, entropic, and surface-energy contributions are shown as solid green, dotted black, and decorated blue lines. The heavy red line shows total $\mu \times 2$ for Si and $\times 200$ for Ge—note the very different scales. All values are relative to the surface average. Vertical lines mark the position of facet edges.

The lateral motion of the two smaller islands in Figs. 1(e)–1(h) is particularly interesting and is highlighted in Fig. 2. These islands lose Ge on the side near the larger island. In the usual case of a stationary island, the island ejects Si from the substrate near its edge to form a trench. Similarly, here the receding island edge ejects Si from the freshly exposed substrate, digging a progressively widening trench. [The broad trench between the larger and smaller islands should really be viewed as two distinct (though overlapping) trenches associated with the respective islands, as is seen in Fig. 3.] Thus both Ge and Si are released simultaneously, from the receding island edge and from the substrate, respectively. The resulting more dilute material is captured in part by the larger island, and in part by the opposite side of the smaller island.

As these islands move laterally, they simultaneously become highly asymmetric, in both composition and shape. The "forward" side is more dilute in composition and more shallow in slope [Figs. 1(g) and 2(c)]. When the island has moved far enough that no Ge-rich core remains, the motion appears to stop.

Exactly these features were observed by Denker *et al.* [5,10]. The experiment found motion directed away from the nearest neighbor. The motion was self-limiting, stopping when the island had moved far enough to dilute its entire volume. The shape of the moving island was asymmetric, as was its composition, with the forward side being more dilute and less steeply sloped. The biggest difference is that in the experiment, the islands were farther apart and more uniform in size. Thus the neighboring island had a much weaker effect. The moving island apparently kept its Ge, simply moving Ge from one side to the other as it captured additional Si during lateral motion. Thus there was substantial net size increase. In our simulation, due to coarsening (loss of material to the larger island), there is little net increase in volume despite the incorporate of Si.

To examine the thermodynamic driving forces, we plot in Fig. 3 the chemical potentials μ_ν for Si and Ge across the surface at a particular moment. Although the morphology is still evolving at this point, the variations in chemical potential across the surface are strikingly small—of order 1 meV for Si. The variations for Ge are much smaller (note the expansion factors for total μ in Fig. 3), because we take the diffusivity to be 50 times larger for Ge than for Si. Thus the distribution of Ge is nearly in equilibrium at any given time, and the evolution is limited by the slower-diffusing species [15]. [The reader should keep in mind that the model here is not a *quantitative* description of any specific

real system, but the values are indicative of general trends for Ge on Si (001) and perhaps also for some III–V systems.]

Figure 3 also shows the decomposition of μ_ν into elastic, entropic, and surface-energy components. These vary individually by much more than does their sum. Strain tends to drive material up from the base to the relaxed top of the island, while surface energy goes the other way, trying to flatten the structure. Both terms vary sharply across the island sidewall. The near cancellation reflects the fact that an island stays close to local equilibrium as it evolves by the slow loss or capture of material, just as was found experimentally [33].

For Ge, Fig. 3 (bottom panel) shows that entropic contributions are even more important than surface energy, though they work together. In opposition to strain, both entropy and surface energy draw Ge into the trench, and both drive Ge away from the island peak, ensuring that the entire surface is covered with an alloyed wetting layer. The surface composition ξ_ν (not shown) is surprisingly uniform, varying by less than $\pm 3\%$ over the entire surface, which must be attributed to the role of entropy.

Only the variations relative to surface-average values are given in Fig. 3. We find that the absolute chemical potential at the surface is reduced by over 50 meV relative to the pure material, due to entropy of mixing [6]. This explains why, even as the trench digs into the Si substrate, it remains lined with Ge. Strain energy tends to drive Ge out of the trench. But the energy scales for Ge wetting, due to both surface energy and entropy of mixing, are much larger than the energy scale for strain.

In conclusion, continuum simulations give considerable insight into the dynamics of strained-layer evolution and quantum-dot formation. We qualitatively reproduce such striking phenomena as trench formation and lateral island motion, and we relate these directly to the thermodynamic driving forces and the constrained dynamics. In the future, it may become possible to extend this approach to more quantitative 3D modeling.

We gratefully acknowledge discussions with A. Rastelli, G. Katsaros, and G. Medeiros-Ribeiro.

[1] See, e.g., references in J. Stangl, V. Holy, and G. Bauer, Rev. Mod. Phys. **76**, 725 (2004).
[2] J. J. Eggleston and P. W. Voorhees, Appl. Phys. Lett. **80**, 306 (2002).
[3] C.-H. Chiu and C. T. Poh, Phys. Rev. B **71**, 045406 (2005).
[4] M. T. Lung, C.-H. Lam, and L. M. Sander, Phys. Rev. Lett. **95**, 086102 (2005).
[5] U. Denker, A. Rastelli, M. Stoffel, J. Tersoff, G. Katsaros, G. Costantini, K. Kern, N. Y. Jin-Phillip, D. E. Jesson, and O. G. Schmidt, Phys. Rev. Lett. **94**, 216103 (2005).
[6] G. Medeiros-Ribeiro and R. S. Williams, Nano Lett. **7**, 223 (2007).
[7] P. B. Joyce, T. J. Krzyzewski, G. R. Bell, B. A. Joyce, and T. S. Jones, Phys. Rev. B **58**, R15981 (1998).
[8] T. I. Kamins, G. Medeiros-Ribeiro, D. A. A. Ohlberg, and R. S. Williams, J. Appl. Phys. **85**, 1159 (1999).
[9] U. Denker, M. Stoffel, and O. G. Schmidt, Phys. Rev. Lett. **90**, 196102 (2003).
[10] G. Katsaros, A. Rastelli, M. Stoffel, G. Isella, H. von Känel, A. M. Bittner, J. Tersoff, U. Denker, O. G. Schmidt, G. Costantini, and K. Kern, Surf. Sci. **600**, 2608 (2006).
[11] I. Goldfarb, Phys. Rev. Lett. **95**, 025501 (2005).
[12] This is generally true in growth by chemical vapor deposition as well; see M. S. Leite, G. Medeiros-Ribeiro, T. I. Kamins, and R. S. Williams, cond-mat/0701710.
[13] J. Erlebacher, M. J. Aziz, A. Karma, N. Dimitrov, and K. Sieradzki, Nature (London) **410**, 450 (2001).
[14] B. J. Spencer, P. W. Voorhees, and J. Tersoff, Phys. Rev. B **64**, 235318 (2001).
[15] J. Tersoff, Appl. Phys. Lett. **83**, 353 (2003); (unpublished).
[16] Y. Tu and J. Tersoff, Phys. Rev. Lett. **93**, 216101 (2004).
[17] B. J. Spencer and M. Blanariu, Phys. Rev. Lett. **95**, 206101 (2005).
[18] We have increased the surface stiffness by a factor of 2 from the value used in Ref. [16].
[19] J. Tersoff, B. J. Spencer, A. Rastelli, and H. von Känel, Phys. Rev. Lett. **89**, 196104 (2002). This model gives a slight curvature rather than true facets, but we refer to "facets" for simplicity.
[20] G. Costantini, A. Rastelli, C. Manzano, R. Songmuang, O. G. Schmidt, K. Kern, and H. von Känel, Appl. Phys. Lett. **85**, 5673 (2004).
[21] J. Tersoff and R. M. Tromp, Phys. Rev. Lett. **70**, 2782 (1993).
[22] D. E. Jesson, K. M. Chen, S. J. Pennycook, T. Thundat, and R. J. Warmack, Phys. Rev. Lett. **77**, 1330 (1996).
[23] Real substrates typically have ample roughness to trigger any instability, even after growth of a "smooth" buffer layer.
[24] R. J. Asaro and W. A. Tiller, Metall. Trans. **3**, 1789 (1972); M. A. Grinfeld, Dokl. Akad. Nauk SSSR **290**, 1358 (1986) [Sov. Phys. Dokl. **31**, 831 (1986)]; D. J. Srolovitz, Acta Metall. **37**, 621 (1989); B. J. Spencer, P. W. Voorhees, and S. H. Davis, Phys. Rev. Lett. **67**, 3696 (1991).
[25] F. M. Ross, J. Tersoff, and R. M. Tromp, Phys. Rev. Lett. **80**, 984 (1998).
[26] A. Rastelli, H. Von Känel, B. J. Spencer, and J. Tersoff, Phys. Rev. B **68**, 115301 (2003).
[27] P. Sutter and M. G. Lagally, Phys. Rev. Lett. **84**, 4637 (2000); R. M. Tromp, F. M. Ross, and M. C. Reuter, Phys. Rev. Lett. **84**, 4641 (2000).
[28] X. Z. Liao, J. Zou, D. J. H. Cockayne, J. Qin, Z. M. Jiang, X. Wang, and R. Leon, Phys. Rev. B **60**, 15 605 (1999).
[29] S. A. Chaparro, Y. Zhang, and J. Drucker, Appl. Phys. Lett. **76**, 3534 (2000).
[30] D. T. Tambe and V. B. Shenoy, Appl. Phys. Lett. **85**, 1586 (2004).
[31] Ph. Sonnet and P. C. Kelires, Appl. Phys. Lett. **85**, 203 (2004).
[32] G. Katsaros *et al.* (unpublished).
[33] A. Rastelli, M. Stoffel, J. Tersoff, G. S. Kar, and O. G. Schmidt, Phys. Rev. Lett. **95**, 026103 (2005).